

# The mode of gas accretion onto star-forming galaxies

Federico Marinacci<sup>1,2</sup>, James Binney<sup>2</sup>, Filippo Fraternali<sup>1</sup>,  
Carlo Nipoti<sup>1</sup>, Luca Ciotti<sup>1</sup>, and Pasquale Londrillo<sup>3</sup>

<sup>1</sup>*Department of Astronomy, University of Bologna, via Ranzani 1, 40127, Bologna, Italy*

<sup>2</sup>*Rudolf Peierls Centre for Theoretical Physics, Oxford University, Keble Road, Oxford OX1 3NP, UK*

<sup>3</sup>*INAF-Osservatorio Astronomico di Bologna, via Ranzani 1, 40127, Bologna, Italy*

Accepted 2010 January 14. Received 2009 December 21; in original form 2009 October 27

## ABSTRACT

It is argued that galaxies like ours sustain their star formation by transferring gas from an extensive corona to the star-forming disc. The transfer is effected by the galactic fountain – cool clouds that are shot up from the plane to kiloparsec heights above the plane. The Kelvin-Helmholtz instability strips gas from these clouds. If the pressure and the metallicity of the corona are high enough, the stripped gas causes a similar mass of coronal gas to condense in the cloud’s wake. Hydrodynamical simulations of cloud-corona interaction are presented. These confirm the existence of a critical ablation rate above which the corona is condensed, and imply that for the likely parameters of the Galactic corona this rate lies near the actual ablation rate of clouds. In external galaxies trails of HI behind individual clouds will not be detectable, although the integrated emission from all such trails should be significant. Parts of the trails of the clouds that make up the Galaxy’s fountain should be observable and may account for features in targeted 21-cm observations of individual high-velocity clouds and surveys of Galactic HI emission. Taken in conjunction with the known decline in the availability of cold infall with increasing cosmic time and halo mass, the proposed mechanism offers a promising explanation of the division of galaxies between the blue cloud to the red sequence in the colour-luminosity plane.

**Key words:** hydrodynamics – turbulence – ISM: kinematics and dynamics – Galaxy: kinematics and dynamics – Galaxy: structure – galaxies: formation – intergalactic medium – cooling flows

## 1 INTRODUCTION

A considerable body of evidence from diverse sources leads to the conclusion that star-forming disc galaxies such as the Milky Way accrete  $\gtrsim 1 M_{\odot}$  of gas each year (e.g. Pagel 1997; Chiappini et al. 2001; Sancisi et al. 2008, and references therein), and have built up their observed discs gradually over the last 10 Gyr (e.g. Twarog 1980; Chiappini et al. 2001; Aumer & Binney 2009). What remains unclear is from what reservoir this gas is drawn, and how it enters the thin gas disc within which stars are formed.

A central question is the temperature of the reservoir: is this low enough ( $T \lesssim 10^4$  K) for the reservoir to contain largely neutral gas, or comparable to the virial temperature,  $T \gtrsim 10^6$  K, of the gravitationally bound groups within which Milky-Way type galaxies currently reside?

In recent years there has been much enthusiasm for so-called cold-mode accretion of gas that has failed to be shock heated to the virial temperature (Birnboim & Dekel 2003; Binney 2004; Keres et al. 2005; Cattaneo et al. 2006; Keres et al. 2009; Hopkins et al. 2009; Law et al. 2009). Cosmo-

logical simulations suggest that cold-mode accretion is the dominant process at redshifts  $z \gtrsim 2$ , but gradually becomes less important. A powerful argument against its currently being the dominant process is the persistent failure of 21-cm surveys to identify significant bodies of intergalactic HI in the nearby Universe (Lo & Sargent 1979; Pisano et al. 2004; Kovac et al. 2009). In particular the Galaxy’s “high-velocity” HI clouds, which as late as 1999 were argued to be distant and massive (Blitz et al. 1999), are now known to be at distances  $\sim 10$  kpc and have masses  $\lesssim 10^5 M_{\odot}$  too small for these clouds to be a cosmologically significant reservoir of gas (Pisano et al. 2004; Wakker et al. 2008; Sancisi et al. 2008).

Spitzer (1956) already inferred from the presence of interstellar absorption in the spectra of high-latitude stars that the Galactic disc must be embedded in pervasive medium of temperature  $\sim 10^6$  K. The empirical case for such “coronal gas” was greatly strengthened by the Copernicus and FUSE missions, which detected ions such as OVI on high-latitude sight lines to distant UV sources, in particular

sight lines that pass close to high-latitude HI clouds (Spitzer & Jenkins 1979; Sembach et al. 2003). The highly ionised gas detected must be collisionally ionised and is most readily interpreted as material at the interface between coronal gas with  $T > 10^6$  K and clouds of cooler, partly neutral HI.

Cosmology strongly suggests that galaxies should be embedded in virial-temperature coronae. First, standard cosmology predicts that only a minority of baryons are contained in stars and cool interstellar gas (e.g. Fukugita & Peebles 2004; Komatsu et al. 2009). In rich clusters of galaxies the “missing” baryons are directly detected through their X-ray emission (Sarazin 2009). In lower-density environments, such as the Local Group, it is thought that the surface-brightness of X-ray emission is too low to be detected by current instrumentation (Rasmussen et al. 2009). Second, three lines of argument indicate that star-formation is an inefficient process in which as much gas is ejected from a star-bursting system as is converted into stars: (i) we actually see winds blowing off star-forming discs (Bland-Hawthorn & Cohen 2003; Strickland et al. 2004); (ii) the spectra of several quasars show blue-shifted absorption-line systems indicative of massive winds flowing away from the star-bursting host galaxy (Pettini et al. 2001; Adelberger et al. 2003); (iii) in clusters of galaxies of order half the metals synthesised by stars are in the intergalactic medium (Sarazin 2009).

Our premise in this paper is that most of the baryons originally associated with the Milky Way’s dark matter comprise a corona of gas at the virial temperature, and that the gas that sustains star formation in the disc is drawn from this corona. The question is how gas makes the transition from a pressure supported corona to the centrifugally supported disc.

For more than thirty years X-ray astronomers have studied the virial-temperature coronae of rich groups and clusters of galaxies. Most of these coronae have central cooling times that are significantly shorter than their ages, and it is natural to ask whether we can understand the Milky-Way’s corona by extrapolating results for cluster “cooling flows” to lower masses. It seems, however that the dynamics of these systems is qualitatively different from the dynamics of the Milky Way’s corona because the central galaxies of rich clusters do not have massive stellar discs. The extent to which gas in rich clusters is cooling (as opposed to radiating) is controversial, but it is now widely accepted that radiative losses by the inner corona are largely offset by mechanical feedback from the central black hole (Binney & Tabor 1995; Omma & Binney 2004; Nipoti & Binney 2005; Best et al. 2007). It is important to understand the origin of this qualitative difference in the dynamics of the coronae of star-forming galaxies of the “blue cloud” and “green valley” in colour-luminosity space (Blanton et al. 2003) and that of the coronae of massive galaxies within the “red sequence”.

Sensitive HI observations of star-forming disc galaxies reveal that these galaxies keep 10 to 25 per cent of their HI a kiloparsec or more above or below their disc plane (Boomsma et al. 2008; Fraternali 2009, and references therein). Most of this gas is thought to have been driven out of the disc by supernova-powered bubbles (Shapiro & Field 1976; Houck & Bregman 1990) and must consist of clouds that are moving on essentially ballistic trajectories because if it were in hydrostatic equilibrium, its vertical density profile would be very much steeper than that observed by virtue

of its low temperature (Collins et al. 2002). The gas is expected to return to the disc within  $\sim 100$  Myr, so the phenomenon of extraplanar HI is evidence for galactic fountains (Bregman & Houck 1997). HI observations of extraplanar gas in the Milky Way are hard to interpret on account of our location within the plane, but the Leiden–Argentina–Bonn (LAB) survey (Kalberla et al. 2005), which mapped local HI emission with high sensitivity, is consistent with the Milky Way having a distribution of extraplanar HI that is similar to the distributions of HI studied around external nearby galaxies.

The extraplanar gas of nearby galaxies has two key properties: (i) the mean rotation speed of the gas declines quite rapidly with distance from the plane; (ii) the gas shows net motion towards the galaxy’s symmetry axis. Fraternali & Binney (2006; hereafter FB06) and Fraternali & Binney (2008; hereafter FB08) fitted models of a galactic fountain to observations of NGC 891 and NGC 2403 and showed that these models can only account for the observed rotation rates and inward motion of the extraplanar gas if the observed HI clouds accrete gas such that the mass of a cloud exponentiates on a timescale  $\sim 650$  Myr. Such an accretion rate simultaneously accounts for data from the two rather different galaxies modelled and yields rates of accretion onto the discs,  $\sim 3.4 M_{\odot} \text{ yr}^{-1}$  and  $0.8 M_{\odot} \text{ yr}^{-1}$  that happen to be similar to the rates at which star-formation consumes gas in these galaxies. The accreted gas is required to have significantly smaller specific angular momentum about the galaxy’s symmetry axis than thin-disc gas.

FB08 suggested that the gas swept up by the fountain’s clouds comes not from the corona but from cool streams embedded within it. They were driven to this conclusion by the shortness of the time it takes coronal gas to flow past a cloud – this time is very much shorter than the cooling time of coronal gas. In this paper we argue that notwithstanding the disparity between the cooling and flow times of the coronal gas, the interaction between a cold cloud and coronal gas leads to cooling of the coronal gas and accretion of it onto the star-forming disc.

In Section 2 we give analytical arguments why cloud-corona interaction must lead to cooling of coronal gas rather than evaporation of HI. In Section 3 we present hydrodynamical simulations of the flow past a cloud, which confirm the analytic arguments. In Section 4 we discuss the implications of these simulations both for further observations and the theory of galaxy formation. Section 5 sums up.

## 2 ANALYTIC ARGUMENTS

### 2.1 Cooling rates

In Model 2 of Fukugita & Peebles (2006), the density of the corona decreases with radius as  $r^{-3/2}$  and at 10 kpc has electron density  $n_e = 2.6 \times 10^{-3} \text{ cm}^{-3}$ . The corona is assumed to be isothermal with  $T_h = 1.8 \times 10^6$  K. Figure 1 shows the cooling time of gas with metallicities  $[\text{Fe}/\text{H}] = -1$  and  $-0.5$  that is in pressure equilibrium with plasma of this temperature and the mean density of this corona between 8 and 12 kpc. At  $T \sim 2 \times 10^6$  K, the cooling time is  $\sim 300$  Myr. Once the temperature has fallen to  $5 \times 10^5$  K, the cooling time has dropped by nearly forty to  $\sim 8$  Myr, which is less than the

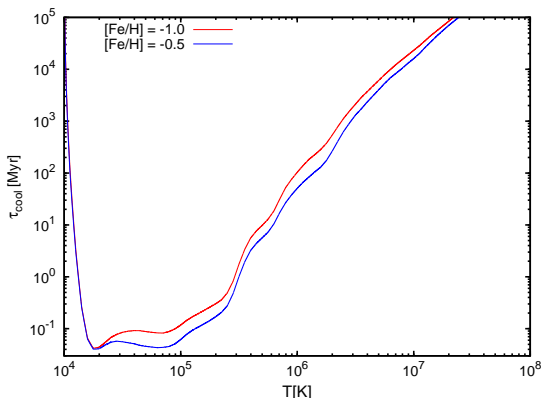


**Figure 1.** Cooling time using Sutherland & Dopita (1993) cooling curve for  $[\text{Fe}/\text{H}] = -1$  and  $-0.5$  for material in pressure equilibrium with coronal gas with  $T = 1.8 \times 10^6$  K and  $n_e = 2.6 \times 10^{-3} \text{ cm}^{-3}$ .

dynamical time at the solar galactocentric radius,  $R_0$ . By the time the temperature has dropped by a further factor of two to  $2.5 \times 10^5$  K, the cooling time has fallen by more than a further order of magnitude and is a mere 0.4 Myr. Thus although the cooling time of ambient gas in the lower corona is long, any diminution in temperature will dramatically shorten the cooling time. In the model of Fukugita & Peebles (2006) the radiating plasma flows inwards at a rate  $\sim 1 M_\odot \text{ yr}^{-1}$ . The work done by compression offsets radiative losses, so the plasma temperature remains  $1.8 \times 10^6$  K.

The mass of an HI halo is rather ill-defined: in an external galaxy it is not clear at what value of  $|z|$  we should place the boundary between disc and halo HI, and in the Galaxy there is a similar ambiguity in the line-of-sight velocity that divides halo from disc HI. If in NGC 891 the disc-halo boundary is conservatively placed at 1.3 kpc, the mass of the HI halo is  $\sim 6 \times 10^8 M_\odot$  (FB06). Kalberla & Dedes (2008) conclude that  $\sim 10$  per cent of the Galaxy’s HI is halo gas, and that the total HI mass within 12 kpc (the region within which most star formation occurs) is  $4.5 \times 10^9 M_\odot$ , so the mass of the HI halo within 12 kpc is  $\sim 4.5 \times 10^8 M_\odot$ .

The HI halo is largely confined to the region  $|z| < 5$  kpc, so we compare the mass of the HI halo at  $R < 12$  kpc to the mass of coronal gas in the cylindrical annulus  $4 \leq R/\text{kpc} \leq 12$ ,  $|z| < 5$  kpc. The coronal mass is  $\sim 2 \times 10^8 M_\odot$ , so within this volume there is over twice as much HI as coronal gas, although the coronal gas will occupy nearly all the space.

The clouds that make up the HI halo typically take 100 Myr to travel from their launch point in the plane through the halo and back to the plane. Consequently, in one Gyr  $\sim 4.5 \times 10^9$  of HI is passed through the  $2 \times 10^8 M_\odot$  of gas in the lower corona. Hence the temperature of the coronal gas would be halved if just 4.5 per cent of the gas that passes through the corona in a Gyr were to mix with the coronal gas. This drop in temperature would bring the cooling time of the coronal gas down to  $\sim 0.1$  Gyr, the local orbital time.

## 2.2 Implications of momentum

The HI clouds of the halo plough through the corona at speeds  $v$  that are less than but comparable to the sound

speed of the coronal gas. Consequently the flow around these clouds is likely to be in a high Reynolds number regime, and each cloud must be decelerated by ram pressure of order  $\rho_h v^2$ , where  $\rho_h$  is the coronal density. In these circumstances the cloud loses its momentum on a timescale equal to  $\rho_c/\rho_h$  times the time  $t_c$  for the cloud to move its own length (FB08). Clouds have diameters of a few tens of parsecs and travel a few kpc, while  $\rho_c/\rho_h \simeq 200$ . Hence clouds must surrender a significant fraction of their momentum to coronal gas (Benjamin 2002). Above we showed that in a Gyr  $\sim 4.5 \times 10^9 M_\odot$  of HI passes through the  $2 \times 10^8 M_\odot$  of the lower corona. Clearly the coronal gas cannot absorb a significant fraction of the momentum of more than 20 times its mass of HI (FB08). Moreover, if the HI disc were losing angular momentum to the corona at the rate this calculation implies, it would be contracting on a Gyr timescale. The natural resolution of these problems is that the disc accretes most of the coronal gas that HI clouds encounter. Then the momentum lost by HI clouds would be returned to the disc, and it would not build up in the corona.

## 2.3 Relation to cooling flows

As was mentioned in Section 1, coronal gas in dark-matter halos more massive than those of spiral galaxies has been extensively studied for four decades. Cooling within these halos shows no tendency to produce a cold stellar disc – the coldest gas is near the centre, where the cooling time is shortest, and whatever gas cools out of the corona feeds the central black hole rather than forming a star-forming disc. The argument of the last subsection may help us to understand why in less massive dark halos cooling coronal gas flows into the disc rather than onto a central black hole: so long as the halo has a star-forming disc, that disc sustains its star formation by reaching up and grabbing coronal gas.

Discs are disrupted by major mergers, which occur rather frequently. Analytic arguments and hydrodynamical simulations of cosmological clustering suggest that when the disc of a relatively low-mass galaxy is disrupted by a major merger, it will quickly re-form from filaments of cold inflowing gas (e.g. Governato et al. 2007). Thereafter it will sustain itself by grabbing coronal gas. When a more massive galaxy experiences a major merger, the disrupted star-forming disc is less likely to re-form. If it does not form from cold inflowing gas, it will not form from coronal gas, because in the absence of a star-forming disc, catastrophically cooling coronal gas will feed the central black hole and reheat the corona. Thus star-formation permanently ceases if there is insufficient cool gas to re-form a star-forming disc after a merger.

In this picture it is likely that cooling at the centre of the corona of a disc galaxy leads to episodic reheating of the central corona, just as in a classical cooling flow. That is, we suggest that the corona of a star-forming disc galaxy accretes onto central black hole *as well as* onto the disc. For this to be a viable proposal, the central reheating associated with accretion by the black hole must not undermine the ability of the star-forming disc to grab coronal gas from the part of the corona that lies above it. This condition could be satisfied if the AGN outburst were sufficiently small and sufficiently directed perpendicular to the galactic plane. This is a topic for a later paper, however.

## 2.4 The wake of a typical cloud

As a cloud moves through the ambient coronal gas, turbulence in the boundary layer at the interface of the hot and cold fluids must cause gas to be stripped from the cloud at some rate. To calculate this rate from ab-initio physics is a daunting task because one would have to consider plasma instabilities in addition to hydrodynamical ones such as the Kelvin-Helmholtz instability, and turbulent energy will be cascading to very small scales. In view of these difficulties, the obvious way forward is to parametrise the problem by hypothesising that mass is stripped from the a cloud of mass  $M_c$  at a rate  $\alpha M_c$ .

A turbulent wake of stripped gas will run back through the corona from the moving cloud. In this wake turbulence will mix the stripped gas with ambient gas. A key quantity is the cooling time of the plasma that results from this mixing. We estimate this under the assumption that mixing occurs so quickly that radiative losses during mixing can be neglected.

Let  $s$  be a short length of the wake, which has cross-sectional area  $A_w$  and originally contained a mass  $A_w s \rho_h$  of coronal gas. In the time  $s/v$  that it took the cloud to pass through the length, a mass  $\alpha M_c s/v$  of gas was stripped from it. After the cold gas has mixed and come into thermal equilibrium with the coronal gas, the temperature of the resulting fluid is

$$T_m = \frac{A_w \rho_h T_h + \alpha M_c T_c / v}{A_w \rho_h + \alpha M_c / v}, \quad (1)$$

where  $T_h$  and  $T_c$  are the coronal and cloud temperatures, respectively.

The natural unit for the cross-sectional area of the wake is the characteristic cross-section  $(M_c/\rho_c)^{2/3}$  of the cloud. We write  $A_w = \beta (M_c/\rho_c)^{2/3}$ , where  $\beta \sim 1$ . Thus

$$T_m = \frac{\beta (M_c/\rho_c)^{2/3} \rho_h T_h + \alpha M_c T_c / v}{\beta (M_c/\rho_c)^{2/3} \rho_h + \alpha M_c / v}. \quad (2)$$

We simplify this expression under the assumption that the cloud is in approximate pressure equilibrium with the corona, so  $\rho_h T_h \simeq \rho_c T_c$ , and have

$$T_m = \frac{1 + (M_c/\rho_c)^{1/3} \alpha / \beta v}{1 + (M_c/\rho_c)^{1/3} (T_h/T_c) \alpha / \beta v} T_h. \quad (3)$$

Since  $(M_c/\rho_c)^{1/3} \alpha / v$  is the fraction of the cloud's mass that is stripped in the time taken for the cloud to travel its own length, and  $\beta \sim 1$ , the second term in the numerator of equation (3) must be small compared to unity and may be neglected. The second term in the denominator is larger by a factor  $T_h/T_c \gtrsim 200$ , so  $T_m$  may be significantly lower than  $T_h$ . On account of the steepness of the cooling-time curve plotted in Fig. 1, this result implies that the cooling time in the wake may fall below the ambient cooling time by a factor of several.

From this back-of-envelope calculation we draw the following conclusions

- Material in the wake will become HI on the timescale that it takes the parent HI cloud to fly its trajectory if the mass-loss rate  $\alpha$  exceeds the critical value

$$\alpha_{\text{crit}} \equiv \frac{\beta v}{(M_c/\rho_c)^{1/3}} \frac{T_c}{T_h}. \quad (4)$$

For  $\beta = 1$  this condition is that in the time taken to travel its own length the cloud lose at least a fraction  $T_c/T_h$  of its mass.

- If the mass-loss rate of clouds falls below this critical value, what mass is stripped from the cloud will be integrated into the corona. This will lower the cooling time of the ambient corona, but not lead to prompt accretion of the wake onto the disc. This drop in the temperature of the corona near the disc will lower the critical mass-loss rate required for subsequent wakes to cool promptly.

- Our estimate of  $\alpha_{\text{crit}}$  was obtained under the assumption that we can neglect cooling during mixing. Although the mixing process is likely to be fast, the cooling rate is extremely large at temperatures that lie within a factor 30 of the cloud's temperature. Hence it is likely that a more exact calculation would produce a lower estimate of  $\alpha_{\text{crit}}$ . We have also neglected compression of the coronal gas as it flows around the cloud. However, the effect of compression on the cooling time of ambient gas is unclear because, while the cooling time decreases with increasing density at constant temperature, it increases with temperature, and compression will be associated with a (largely adiabatic) rise in  $T$ .

- The effective value of  $\beta$  is uncertain. On one hand, as the simulations will show, the cloud flattens in its direction of motion, making  $\beta > 1$ . On the other hand, the distribution of cloud material is likely to be concentrated in a network of thin sheets. The effective value of  $\beta$  for an individual sheet could be small.

- Dimensional analysis indicates that  $\alpha$  will lie near  $\alpha_{\text{crit}}$ : the rate of stripping is essentially determined by the rate at which coronal gas hits the leading surface of the cloud and strips a comparable mass from the cloud. Quantitatively,  $\alpha M_c \equiv \dot{M} = -b\pi r^2 \rho_h v$ , where  $b \sim 1$ . When we eliminate  $r$  and  $\rho_h$  in favour of  $M_c$  and  $T_h$  we find that the characteristic mass-loss parameter is

$$\alpha = \left(\frac{9\pi}{16}\right)^{1/3} \frac{b}{\beta} \alpha_{\text{crit}}. \quad (5)$$

- If we take the mass-loss rate to be given by the previous item, we find that the mass of a cloud that will completely mix with the corona after travelling distance  $L$  is

$$M_{\text{crit}} = \frac{9\pi}{16} \left(\frac{T_c}{T_h} bL\right)^3 \rho_c. \quad (6)$$

Equivalently, the distance travelled prior to destruction is predicted to be  $\sim T_h/T_c$  times the size of the cloud.

## 3 NUMERICAL SIMULATIONS

Numerical simulations of a cloud of gas at  $T \sim 10^4$  K moving through coronal gas at an initial speed  $v_0 \sim 75 \text{ km s}^{-1}$  will illustrate these points and give insight into both typical mass-loss rates and the critical mass-loss rate required for prompt cooling of the wake. The simulations are idealised in that they neglect gravitational acceleration and the variation of the coronal density along the cloud's trajectory. However, the galactocentric radius of the clouds varies by  $\lesssim 30$  per cent, so the density variation is not extreme. The range of relevant velocities depends on the extent to which

the corona corotates with the disc, which is currently unclear. The velocity we have chosen to explore is at the low end of the relevant range because it is of order the velocity at which clouds have to be ejected from the disc in order to reach heights of a few kiloparsecs. Larger velocities would clearly lead to more rapid interaction with the corona than that explored here.

It is important to be clear about what can and cannot be learnt from the simulations. First any simulation incorporates limited physics and limited spatial resolution. In the real world the fluid is a magnetised, almost perfectly conducting, largely collisionless plasma. The shear flow at the cloud-corona interface will draw out and strengthen the field lines originally in the plasma. This drawing out will make the velocity distribution of particles anisotropic, which will excite plasma instabilities. These instabilities will both heat and mix the plasma. By contrast the tendency of the field lines to follow stream lines will strongly inhibit mixing. None of this complex physics is included in our simulations.

Instead, in the simulations ablation and mixing are driven by the Kelvin-Helmholtz instability, which gives rise to ripples in the fluid interface. These ripples develop into vortices, which shed smaller vortices, which themselves shed vortices. In a numerical simulation numerical viscosity prematurely truncates this hierarchy of vortices on a scale of a few times the grid spacing  $\Delta$ . On scales finer than  $\Delta$ , the fluid is represented as perfectly mixed, whereas it is in reality a roughly fractal foam of high- and low-density regions. The condition for the simulations to be a reliable guide to the large-scale structure of the flow is that the large-scale dynamics of this foam is equivalent to the dynamics of the locally homogeneous fluid that is actually represented. This is a reasonable proposition, but we have to expect that the values of the flow's macroscopic parameters, such as ambient pressure and cooling rate, at which a simulation of given resolution most closely approximates reality are likely to vary with resolution. That is, we anticipate a phenomenon analogous to renormalisation in quantum field theory, where the appropriate value of the bare electron mass, for example, is a function of the largest wavenumber summed over.

The simulations do not include thermal conduction. On the smallest scales conduction must play an important role in homogenising a mixture of cloud and coronal gas, and in the simulations this role is effectively covered by numerical mixing and diffusion. Consequently, our failure to model thermal conduction is most worrying on intermediate and larger scales. In a magnetised plasma heat is largely conducted along field lines. The field lines in upstream ambient gas are inevitably disconnected from field lines in the cloud. Any connection between these sets of field lines must occur in the turbulent wake. This fact is likely to severely limit the effectiveness of thermal conduction.

The physical properties of the clouds and the corona considered here are such that the clouds would be stable against conductively-driven evaporation if they were stationary (see Nipoti & Binney 2007), so it is very unlikely that conduction plays an important role in the energetics of our problem. In principle conduction lowers the rate at which a moving cloud is ablated, by damping the Kelvin-Helmholtz instability (Vieser & Hensler 2007), but this effect will be unimportant if conduction is magnetically suppressed to values small compared to the Spitzer or saturated values.

In light of these remarks, the aims of the simulations are as follows

- To estimate the mass-loss rate  $\alpha$  for comparison with  $\alpha_{\text{crit}}$ . It is advantageous to do this in the absence of radiative cooling for then (a) the calculations are slightly faster, and (b) one can identify the cloud with gas at  $T \lesssim 10^5$  K since any ablated material will be heated to and remain at higher temperatures. We will show that the mass-loss rate is reasonably independent of  $\Delta$ .
- To show that for any given metallicity of the gas, there is a critical ambient pressure  $P_{\text{crit}}$  above which the mass of cool gas increases with time through condensation in the wake and below which the wake tends to evaporate. We shall find that although our values of  $P_{\text{crit}}$  vary with both metallicity and  $\Delta$ , they lie within the range of values that occur in practical cases. Hence it is plausible that the true value of  $P_{\text{crit}}$  lies below the actual ambient pressures, so real wakes give rise to condensation and accretion.

### 3.1 The simulations

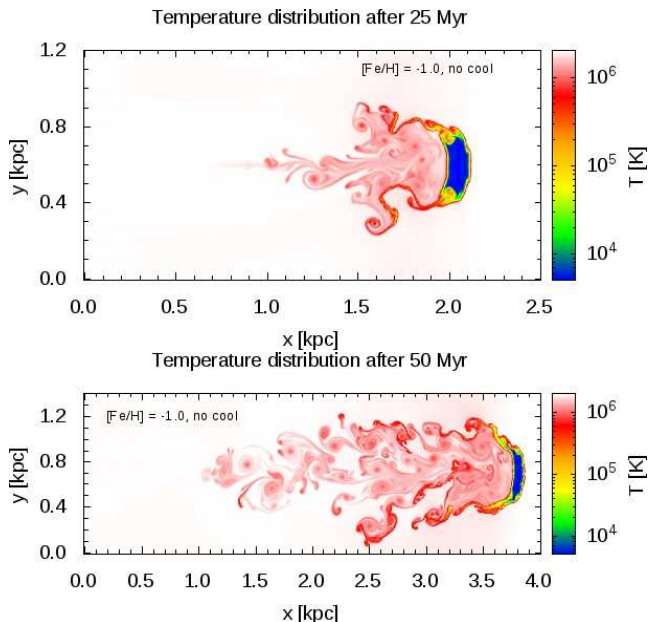
The parameters of the simulations are listed in Table 1. In all simulations the initial cloud velocity was  $75 \text{ km s}^{-1}$  and the initial radius was 100 pc. The temperature of the corona is restricted to a narrow range around  $2 \times 10^6$  K by the requirement that the corona be bound to the Galaxy and yet be extensive enough to contain a cosmologically significant mass (Fukugita & Peebles 2006, e.g.), so in all simulations we made the corona's temperature  $2 \times 10^6$  K. In simulations of the low-pressure sequence the total particle density of the corona was  $10^{-3} \text{ cm}^{-3}$  (except in the Z6 simulation in which it was reduced to  $4 \times 10^{-4} \text{ cm}^{-3}$ ), implying  $n_e \simeq 0.5 \times 10^{-3}$ , while in the high-pressure simulations it was twice as great. These values are both lower than the density  $n_e = 2.6 \times 10^{-3} \text{ cm}^{-3}$  at  $r = 10 \text{ kpc}$  in model 2 of Fukugita & Peebles (2006), and may be compared with the total particle density  $n = 4 \times 10^{-4}$  at 10 kpc above the plane adopted by Heitsch & Putman (2009). In all but two simulations the initial cloud temperature was  $10^4$  K; in the last two (high-pressure) simulations the cloud temperature was lowered to  $5 \times 10^3$  K since at the higher temperature (and therefore lower density contrast) the cloud was totally disrupted by 50 Myr. The cloud mass ranged from 0.44 to  $4.4 \times 10^4 M_\odot$  depending on the pressure of the corona and the temperature of the cloud. The Jeans mass of the standard cloud ( $r = 100 \text{ pc}$ ,  $T_c = 10^4 \text{ K}$ ) is  $1.6 \times 10^8 M_\odot$  so our neglect of self gravity is amply justified.

The calculations were performed on two-dimensional, Cartesian grids of three sizes:  $384 \times 768$  (c),  $512 \times 1024$  or  $1536$  for simulations run to 50 Myr (m), and  $768 \times 1536$  (f). Ghost cells are used to ensure that the pressure gradient vanishes at the grid boundaries. Every configuration was simulated twice, once with cooling on and once with cooling off. When radiative cooling is permitted, it follows the prescription of Sutherland & Dopita (1993). The metallicity of the cloud is always the same as that of the ambient medium, and is varied from zero up to solar. We used the Eulerian code ECHO, which is flux-conserving and uses high-order shock-capturing schemes; a detailed description and tests of it can be found in Londrillo & Del Zanna (2004).

Since one of the dimensions perpendicular to the cloud's

**Table 1.** Parameters of the simulations. The grids sizes are coarse (c)  $384 \times 768$ , medium (m)  $512 \times 1024$  or  $1536$  depending on duration, and fine (f)  $768 \times 1536$ . Each configuration is simulated both with and without radiative cooling.

simulation	time [Myr]	[Fe/H]	$T_h$ [K]	$n_h$ [ $\text{cm}^{-3}$ ]	$T_c$ [K]	$M_c$ [ $10^4 M_\odot$ ]	grid size
Low-pressure simulations							
Z_0	25	no met.	$2 \times 10^6$	$10^{-3}$	$10^4$	1.1	c,m,f
Z_1	25	-3.0	$2 \times 10^6$	$10^{-3}$	$10^4$	1.1	c,m,f
Z_2	25	-2.0	$2 \times 10^6$	$10^{-3}$	$10^4$	1.1	c,m,f
Z_3	25	-1.5	$2 \times 10^6$	$10^{-3}$	$10^4$	1.1	c,m,f
Z_4	25	-1.0	$2 \times 10^6$	$10^{-3}$	$10^4$	1.1	c,m,f
Z_5	25	-0.5	$2 \times 10^6$	$10^{-3}$	$10^4$	1.1	m,f
Z_6	25	0.0	$2 \times 10^6$	$4 \times 10^{-4}$	$10^4$	0.44	m
High-pressure simulations							
T_4_Z_3	25	-1.5	$2 \times 10^6$	$2 \times 10^{-3}$	$10^4$	2.2	m
T_4_Z_4	50	-1.0	$2 \times 10^6$	$2 \times 10^{-3}$	$10^4$	2.2	m
T_3_Z_4	50	-1.0	$2 \times 10^6$	$2 \times 10^{-3}$	$5 \times 10^3$	4.4	m

**Figure 2.** The temperature distribution after 25 and 50 Myr when radiative cooling is switched off. The computational grid has medium resolution (see table 1), the initial cloud temperature was  $5 \times 10^3$  K and the coronal density was  $2 \times 10^{-3} \text{ cm}^{-3}$ .

velocity has been suppressed, we are in effect simulating flow around an infinite cylindrical cloud that is moving perpendicular to its long axis. The cylinder initially has a circular cross section of radius  $r$ . From the simulations we obtain quantities per unit length of the cylinder. We relate these to the corresponding quantities for an initially spherical cloud of radius  $r$  by multiplying the cylindrical results by the length  $\frac{4}{3}r$  within which the mass of the cylinder equals the mass of the spherical cloud.

### 3.2 Flows without radiative cooling

We first study the simulated flows in the absence of radiative cooling, in order to assess the importance of the limited resolution of the simulations.

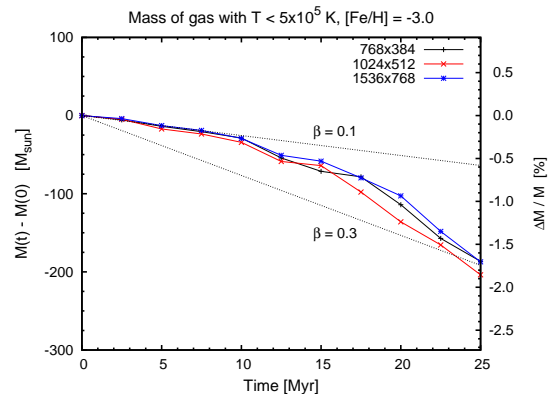
**Figure 3.** The evolution of the mass of gas at  $T < 5 \times 10^5$  K for three different resolutions when radiative cooling is switched off. The dotted straight lines show the effect of the critical mass-loss rate  $\alpha_{\text{crit}}$  for two values of  $\beta$ . The particle density of the corona is  $10^{-3} \text{ cm}^{-3}$ .

Figure 2 shows the temperature distribution on the grid after 25 Myr and 50 Myr with radiative cooling turned off. The cloud has been flattened into a pancake by ram pressure from the medium it is moving into. The shear flow over the leading face of the pancake is causing vortices to be shed from the pancake's edges that are analogous to the vortices shed by an aeroplane wing. In the highly turbulent wake behind the cloud, the temperature fluctuates around  $10^6$  K depending on the fraction of the gas in each cell that comes from the cloud rather than the corona.

Figure 3 quantifies the speed at which ablation reduces the cloud's mass by plotting the mass of gas below  $5 \times 10^5$  K versus time for simulations of three resolutions. We see that over 25 Myr  $\sim 200 M_\odot$  of gas ( $\sim 2$  per cent of the cloud's mass) are heated to above  $5 \times 10^5$  K, regardless of the grid resolution; it seems that even the coarsest grid has sufficient resolution to model satisfactorily the stripping of gas from the leading edge of the cloud. In the absence of radiative cooling, any gas that is stripped from the cloud will eventually be heated to above  $5 \times 10^5$  K as it mixes with coronal gas. The details of the smallest vortices involved in the mixing process are resolution-dependent in the sense that at



higher resolutions some gas remains cold for slightly longer before numerical mixing on the grid scale eliminates it. The cloud's mass-loss rate is resolution-independent because all stripped gas will be heated within a couple of large-scale eddy-turnover times, regardless of resolution.

The mass-loss rate increases gently with time because it depends on the area of the cloud's leading face, which increases with time as the cloud is squashed into a thinner and thinner pancake, a process that is apparent in Fig. 2.

The dotted straight lines in Fig. 3 show the critical mass-loss rate defined by equation (4) for  $\beta = 0.1$  and  $0.3$ . We see that, as predicted above on dimensional grounds, the measured mass-loss rate lies near  $\alpha_{\text{crit}}$ . Actually the simulations must underestimate  $\dot{M}_c$  because mass is lost from the cloud's edges, which have total length  $\frac{8}{3}r$  in cylindrical geometry and  $2\pi r$  in the spherical case. Thus we expect the numerical rates to be  $\sim 0.42$  of the true rate and in three dimensions  $\beta$  would lie close to unity.

These results enable us to estimate the minimum size that a cloud must have if it is to survive a typical passage through the corona. From Fig. 10 of FB06 we have that trajectories last 100 Myr, and in this time a cloud travelling at  $v \sim 70 \text{ km s}^{-1}$  will move 7 kpc. Setting  $L = 7 \text{ kpc}$  and  $b = 1$  in equation (6) we find that clouds with masses less than

$$M_{\text{crit}} = 220 \left( \frac{L}{7 \text{ kpc}} \right)^3 \left( \frac{T_h/T_c}{200} \right)^{-2} \left( \frac{n_h}{10^{-3} \text{ cm}^{-3}} \right) M_{\odot} \quad (7)$$

will completely mix with the corona before they can return to the plane.

It is important to know how the mass-loss rate scales with cloud mass and thus cloud radius. Since mass is lost from the leading surface of the cloud, we would expect the absolute mass-loss rate to scale as  $\dot{M}_c^{2/3}$  and therefore the specific mass-loss rate  $\alpha \propto \dot{M}_c^{-1/3}$ . We have verified this dependence by simulating the evolution of a cloud of the standard density but radius doubled to 200 pc.

### 3.3 Flows with radiative cooling

When radiative cooling is switched on, the strength of the dependence of the cooling rate upon  $T$  that is apparent in Fig. 1, substantially increases the difficulty of the simulations and the uncertainties surrounding their results because now the structure of the turbulent wake is crucial. Indeed, evaporation is favoured over cooling by more effective dispersal of stripped material through a large volume of the corona. The higher the resolution delivered by the code, the greater the dynamic range of the hierarchy of vortices, and the more effective is the dispersal of stripped material, with the consequence that increased resolution favours evaporation over condensation.

Each panel of Fig. 4 is the analogue of Fig. 3 but with radiative cooling turned on; in the three panels the metallicity increases from zero (top panel) through  $[\text{Fe}/\text{H}] = -1$  (middle panel) to  $-0.5$  (bottom panel). The simulations with  $[\text{Fe}/\text{H}] < -1$  do not differ significantly from that at zero metallicity. In all three panels the mass of cool gas starts by increasing rather than decreasing, and the rate of increase naturally increases with metallicity. When  $[\text{Fe}/\text{H}] = -0.5$ , the increase continues throughout the 25 Myr simulated, but at lower metallicities the mass of cool gas eventually starts

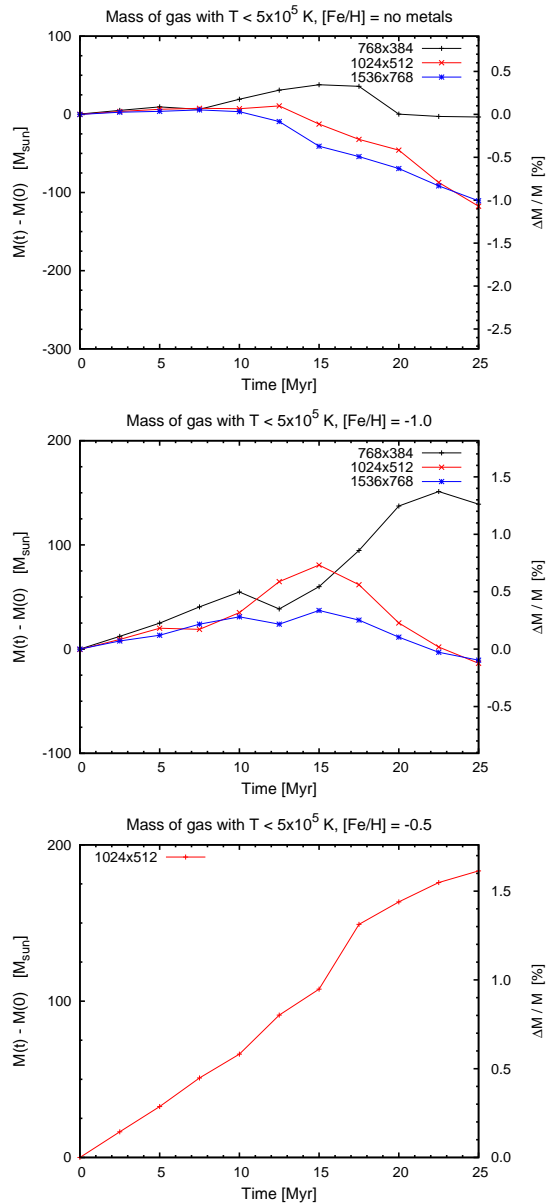


**Figure 4.** The same as Fig. 3 but with radiative cooling turned on. In the top panel the plasma has primordial abundances, while in the middle and bottom panels  $[\text{Fe}/\text{H}] = -1$  and  $-0.5$ , respectively. In all three panels the corona had particle density  $10^{-3} \text{ cm}^{-3}$ .

to decrease. As anticipated, the results are unfortunately dependent on numerical resolution: in general there is a tendency for the mass of cool gas to decrease as the resolution increases, although the medium and high-resolution simulations give rather similar results.

Figure 5 shows the effect of doubling the particle density of the corona to  $2 \times 10^{-3} \text{ cm}^{-3}$ : even at metallicity  $[\text{Fe}/\text{H}] = -1$  the mass of cool gas now increases throughout the 50 Myr simulated, and in fact in the latter half of the simulation cold gas accumulates at an accelerating rate. This result should be contrasted with that shown by the middle panel of Fig. 4, which shows that at the same metallicity but half the density, the mass of cool gas starts to decrease after  $\sim 15$  Myr. If we extrapolate the behaviour shown in Fig. 5

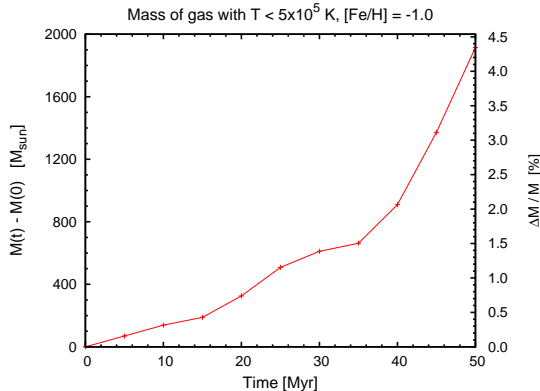


**Figure 5.** The mass of gas at  $T < 5 \times 10^5$  K in a simulation with coronal particle density  $2 \times 10^{-3} \text{ cm}^{-3}$  and metallicity  $[\text{Fe}/\text{H}] = -1$ .

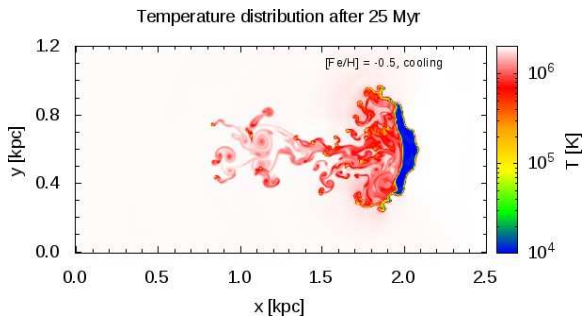


**Figure 6.** As Fig. 2 but with the coronal density lowered to  $10^{-3} \text{ cm}^{-3}$  and radiative cooling turned on. The metallicity is  $[\text{Fe}/\text{H}] = -0.5$ .

to the whole Milky Way halo, assuming as its total mass the value given in Sect. 2.1, we obtain a global accretion rate of  $\approx 0.5 M_{\odot} \text{ yr}^{-1}$ .

Figure 6 shows the temperature distribution at  $t = 25$  Myr in a simulation with cooling of plasma with  $[\text{Fe}/\text{H}] = -0.5$  and ambient particle density  $10^{-3} \text{ cm}^{-3}$ . Comparing this figure with the upper panel of Fig. 2 we see that cooling makes the wake longer and less laterally extended. We have also run simulations with lower values for the coronal gas density and found that accretion is still present for  $n_{\text{h}} \gtrsim 4 \times 10^{-4} \text{ cm}^{-3}$  provided that the metallicity is about solar.

Figure 7 shows for the high-pressure simulation T\_3\_Z\_4 the distribution of cool gas along the cloud’s direction of travel (top panel) and its distribution in velocity along the same direction (bottom panel) at the start of the simulation (black curve) and after 50 Myr when radiative cooling is (blue curve) or is not (red curve) included. From the upper panel we clearly see the effectiveness of cooling in enhancing the mass of cool gas. We also see that  $\lesssim 1$  percent of the cold gas lies more than 1 kpc behind the cloud. In the lower panel around  $75 \text{ km s}^{-1}$  we clearly detect the deceleration of the main body of the cloud, but more striking is the width of the velocity range over which small amounts of cool gas are distributed. A few times  $100 M_{\odot}$  is accelerated to higher velocities than the cloud’s. A slightly larger mass of gas is decelerated to negative velocities. This velocity distribution

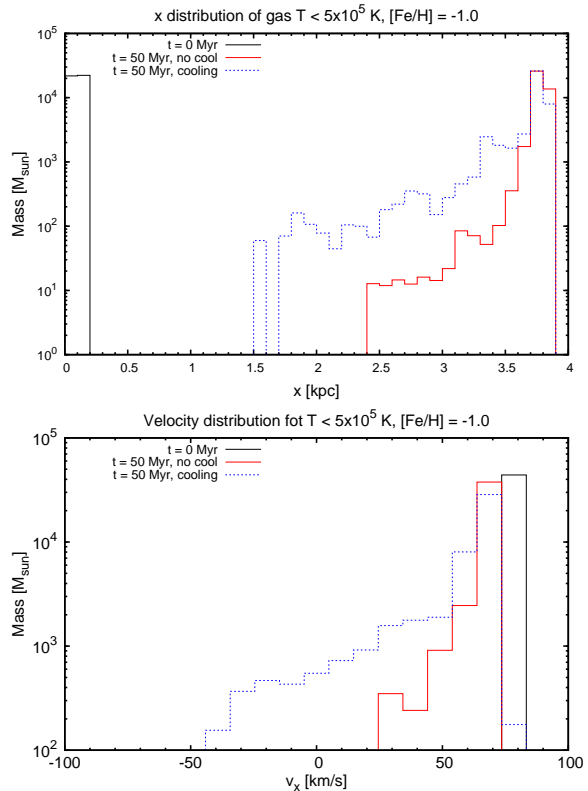


**Figure 7.** Upper panel: the distribution of cool gas along the cloud’s direction of travel. The black curve shows the initial distribution while the blue dotted curve and red solid curve show the distributions at  $t = 50$  Myr with and without radiative cooling, respectively. Lower panel: the same but for the velocity along the direction of travel.

implies that gas circulates around vortices at speeds that are comparable to the speed of the cloud’s forward motion.

Figure 8 shows the distribution of cold gas in  $x$ , the direction of travel, and in  $v_x$  for the high-pressure simulation T\_3\_Z\_4 with and without cooling. Turning on cooling greatly broadens the extent in both  $x$  and  $v_x$  of low-density cool gas. In both simulations, the region of highest gas density runs from  $70 \text{ km s}^{-1}$  at the cloud’s location down to  $\sim 20 \text{ km s}^{-1}$  0.5 kpc behind the cloud. Thus hydrodynamics leads to a steep velocity gradient,  $\sim 80 \text{ km s}^{-1} \text{ kpc}^{-1}$  in the part of the wake that will dominate 21-cm emission. Jin & Lynden-Bell (2007) assume that a gradient in the measured line-of-sight velocity along Complex A,  $\sim 12 \text{ km s}^{-1} \text{ kpc}^{-1}$ , is entirely produced by the Galaxy’s gravitational field. In light of our simulations this assumption should be treated with some caution.

The lower panel of Fig. 8 shows that the velocity width of the wake increases with distance from the cloud for  $\sim 800 \text{ pc}$  from the cloud as a result of the lower envelope (velocities in the opposite direction to the cloud’s motion) moving downward towards  $-100 \text{ km s}^{-1}$ , while the upper boundary remains at  $\sim 90 \text{ km s}^{-1}$ . This is further evidence that turbulent eddies impart peculiar velocities comparable to the cloud’s velocity. Just behind the cloud material has to flow faster than the cloud in order to flow into the space vacated as the cloud moves on. Further back similar vortices



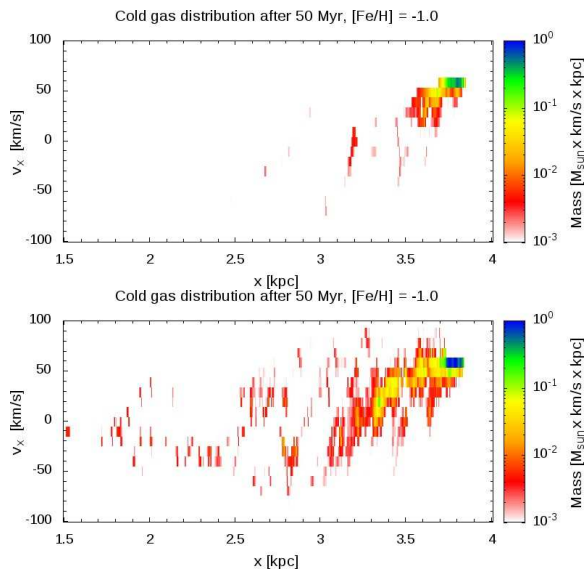


**Figure 8.** Distribution of velocities as a function of distance down the wake in T<sub>3</sub>Z<sub>4</sub> at 50 Myr when cooling is switched off (upper panel) and on (lower panel)

carry cold gas away from the cloud with similar velocities. In the region 1 to 2 kpc behind the cloud, the turbulence damps quite rapidly.

From these simulations we conclude the following.

- There is clear evidence that the simulations’ limited resolution is adequate for determining the rate at which gas is stripped from a cloud, although the two-dimensional nature of the simulations suggests that they will underestimate the stripping rate by a factor  $\sim 2$ .
- The stripping rate tends to increase with time as a result of the cloud being flattened by ram pressure.
- The stripping rate is best determined from simulations in which cooling is turned off, and it is found to lie close to the rate expected on dimensional grounds. In §2 we saw that this rate is very similar to the critical rate at which cooling takes over from evaporation.
- Whether stripped gas is evaporated or leads to the condensation of coronal gas depends on the structure of the turbulent wake. Consequently the finite spatial resolution of the simulations makes it impossible to determine with confidence the combinations of pressure and metallicity which divide evaporation from condensation. However the simulations confirm analytic arguments, which imply that for a given cloud there is a critical path in the space spanned by the coronal pressure and metallicity which divides situations in which, at high pressure or metallicity, coronal gas condenses in the wake and those in which, at lower pressure or metallicity, the gas stripped from the cloud is evaporated by the corona. Both the simulations and analytic arguments suggest that the parameters of the Galactic corona lie close to this critical path.
- The neutral gas that trails the cloud is strongly influenced by hydrodynamics forces and cannot be considered to be on an orbit. There is a large velocity gradient along its high-density ridge in velocity-position space. Within  $\sim 2$  kpc

from the cloud the velocity width of the stream is of order of the cloud’s velocity.

## 4 DISCUSSION

The picture developed here of the connection between the Galactic fountain and accretion onto the star-forming disc differs materially from that proposed by FB08: in that paper HI clouds grew in mass as they moved through the corona; here each cloud loses mass, but the mass of cold gas in a cloud and its wake taken together increases with time. A natural question is whether the present picture predicts a similar overall picture of 21-cm emission to that proposed by FB08. If it does, it will fit the data reasonably well.

FB08 fitted 21-cm data cubes for NGC 891 and NGC 2403. Individual clouds are for the most part not resolved in these data, so the observed emission is due to many superposed clouds. In the FB08 model, each cloud places a blob of emission in the cube, centred on its sky-position and line-of-sight velocity, and smeared by the angular and velocity resolution of the survey. If the picture developed here is correct, the emission of each cloud is extended in velocity and is elongated on the sky. Very sensitive 21-cm data would be required to see the full extent of the trail of an individual cloud – the antenna temperature will drop by two orders of magnitude within 0.5 kpc and  $\sim 25 \text{ km s}^{-1}$  of the cloud’s position and velocity. However, the integrated emission from many individually undetectable trails must contribute to the HI “beards” of nearby galaxies. In a forthcoming study we will modify the pseudo-data cubes of FB08 to include the extended emission from the trails of clouds. We suspect that these improved data cubes will have similar observable properties to those of FB08 because the velocity centroid of each cloud’s total emission will be unchanged.

Clearly it is to surveys of our own Galaxy that we must turn for evidence that clouds have HI-rich wakes. Maps of the 21-cm emission of individual high-velocity clouds generally display a tadpole-like structure: the cloud is elongated and the point of highest surface brightness lies towards one end (e.g. Brüns et al. 2001; Westmeier et al. 2005). In the scenario proposed here, tadpole-like structures can be explained by the interaction between the cloud and the ambient (coronal) medium. This interaction leads to the formation of trailing material behind the cloud.

Even in our Galaxy most emission from extraplanar gas is unresolved in the sense that along any direction in the LAB survey, emission is detected over a wide band in velocity around 0. However, a scan through the data cube, one heliocentric velocity at a time, reveals numerous elongated structures along which there is a systematic trend in velocity. These could well be the wakes of relatively massive clouds.

Clouds with masses well below the threshold for detection of their 21-cm emission can be detected through the absorption lines to which they give rise in the ultraviolet spectra of background sources. Absorption-line studies suggest that large HI complexes are associated with numerous small HI clouds (Richter et al. 2005). Could these small clouds be the knots of cold gas visible in the wake of Fig. 6? If this interpretation is correct, the small clouds would be found only on one side of the large complex, and they would

have a mass spectrum that was restricted to masses very much smaller than that of the complex.

In the simulations the metallicity of the cloud is the same as that of the corona, whereas real-world clouds will be more metal-rich than the corona by a factor up to 10. Whether gas condenses or evaporates depends on the cooling rate of gas that is roughly a 50–50 mixture of gas stripped from the cloud and coronal gas, so the most realistic simulations are those in which the universal metallicity is about half that of real clouds; that is the simulations with  $[\text{Fe}/\text{H}] \sim -0.5$ .

We must obviously ask how valid a guide two-dimensional simulations will be to the real, three-dimensional problem. Reducing the dimensionality of the problem reduces the number of high-wavenumber modes relative to the immediately driven low-wavenumber modes, thus making the power-spectrum of turbulence less steep. This argument suggests that turbulent mixing will be more effective in two dimensions than in three, with the consequence that our simulations have a tendency to overestimate the pressure or metallicity of the transition from evaporation to condensation. However, this conclusion must be considered very tentative at this time.

#### 4.1 Relation to prior work

The ablation of clouds that move through a low-density medium has been discussed by, among others, Murray et al. (1993), Dunge (1997), Vieser & Hensler (2007) and Heitsch & Putman (2009). In addition to studying the ablation of pressure-bounded clouds as here, some of these authors have considered also gravitationally bound clouds and included thermal conduction in addition to radiative cooling. Vieser & Hensler (2007) find that thermal conduction stabilises a moving cloud by reducing the magnitude of the velocity gradient in the boundary layer where the cloud meets the ambient medium; a smaller velocity gradient leads to slower growth of the Kelvin-Helmholtz instability.

Most previous simulations assume the flow to be axisymmetric around the velocity of the cloud’s motion. In such simulations material becomes trapped on the assumed symmetry axis, where the radial velocity must vanish by symmetry. Murray et al. (1993) also simulated clouds with the symmetry assumed here and found that the main results were independent of the adopted geometry.

Murray et al. (1993) found ablation to proceed faster than we do and interpreted their ablation timescale as the inverse of the Kelvin-Helmholtz growth rate, which is larger than  $\alpha_{\text{crit}}$  by  $\sim (T_{\text{h}}/T_{\text{c}})^{1/2}$ . The difference between their ablation rate and ours probably arises from their use of a different criterion for identifying cloud gas: they took this to be the mass within an appropriate sphere, whereas we have defined cloud gas to be cool gas, regardless of where it resides. In other respects our results are in accordance with earlier findings.

The simulations most comparable to ours are those of Heitsch & Putman (2009), who simulated the ablation of cool clouds that fall towards the disc through the corona. Consequently, their characteristic coronal density,  $n_{\text{h}} \simeq 10^{-4} \text{ cm}^{-3}$ , was a factor 2 to 4 lower than ours. Their simulations used a three-dimensional grid, so their grid spacing was coarser and they could not provide evidence of numerical

convergence. Their clouds, which had similar initial masses to ours, fragmented in a similar fashion. In most simulations the total mass of HI in the computational volume declined with time, although in some simulations an upturn in the HI mass is evident at late times as the cloud approaches the plane. Our numerical results are entirely consistent with theirs, although our physical motivation is different and, crucially, our parameter regime extends to the higher coronal densities expected near the plane.

Recent attempts to model extraplanar HI include those of Barnabe et al. (2006) and Kaufmann et al. (2006). Barnabe et al. (2006) investigated the equilibria of differentially rotating distributions of gas in flattened gravitational potentials. They showed that by making the specific entropy and angular momentum of the gas vary appropriately within the meridional plane, the kinematics of the gas can be made consistent with the data for HI around NGC 891. They noted that dynamical equilibrium required the gas to be too hot to be neutral, so the gas within their model could not be the observed as HI itself, but suggested it might be coronal gas within which HI clouds were embedded as almost stationary structures (see also Marinacci et al. 2009).

Kaufmann et al. (2006) studied the settling of hot gas within the gravitational potentials of spherical galaxy-sized dark halos. The gas was initially spinning with a rotation velocity that was independent of radius (so specific angular momentum  $j \sim r$ ). A prompt cooling catastrophe caused cold gas to accumulate in a centrifugally supported disc, and clouds of cold gas were subsequently seen to be falling through hotter gas towards this disc. This simulation is interesting but one has to worry that the cool clouds are numerical artifacts. It is well known that standard smooth-particle hydrodynamics artificially stabilises contact discontinuities (Agertz et al. 2007; Price 2008). Moreover, observed high-velocity clouds all have masses that lie below the resolution limit of the simulations of Kaufmann et al., so the clouds they see have no counterparts in reality. Finally, Binney et al. (2009) showed that unless the specific entropy profile of coronal gas is unexpectedly flat, a combination of buoyancy and thermal conductivity (which was not included in the Kaufmann et al. simulations) suppresses thermal instability.

## 5 CONCLUSIONS

There is abundant evidence that in galaxies like ours, star-formation powers a fountain that each gigayear carries  $\gtrsim 5 \times 10^9 M_{\odot}$  of HI to heights in excess of 1 kpc above the plane. Several lines of argument strongly suggest that galaxies like ours are surrounded by gas at the virial temperature – coroneae. The density of the corona, which must vary with position, is very uncertain, especially in the region above the star-forming disc. However, there are indications that this density is such that the local coronal cooling time is of order a gigayear. At least half of the baryons in the Universe are believed to reside in coroneae and their extensions to intergalactic space.

Models of the chemistry and stellar content of the Galactic disc require the disc to accrete  $\gtrsim 1 M_{\odot} \text{ yr}^{-1}$  of low-metallicity gas. The corona is the only reservoir of baryons that is capable of sustaining an infall rate of this order for

a Hubble time. Therefore there is a strong *prima-facie* case that star formation in the disc is sustained by cooling of coronal gas.

The dynamical interaction of HI clouds of the fountain with coronal gas is inevitable. For any plausible coronal density, the ram pressure arising from motion through the corona leads to non-negligible loss of momentum by fountain clouds. If this momentum were retained by the corona rather than returned to the disc, the corona would rapidly become rotation-dominated. We have not pursued this possibility because we think it is more likely that coronal gas that absorbs momentum from fountain clouds is shortly thereafter accreted by the disc. We suggest that the absorption proceeds as follows: (i) coronal gas strips gas from the leading edge of the cloud as a result of Kelvin-Helmholtz instability; (ii) in the turbulent wake of the cloud, the stripped gas mixes with a comparable mass of coronal gas; (iii) as a result of this mixing the cooling time becomes shorter than the cloud’s flight time and coronal and stripped gas together form knots of HI that trail behind the cloud and fall onto the disc within a dynamical time. This scenario is suggested by a combination of analytic and observational arguments, and supported by hydrodynamical simulations.

Analytic arguments imply that for a given coronal pressure and metallicity there is a critical rate of mass loss by a cloud,  $\alpha_{\text{crit}}$ , such that at lower mass-loss rates, stripped gas will be evaporated by the corona, and the total mass of HI will decrease during a cloud’s flight. By contrast, when the mass-loss rate exceeds  $\alpha_{\text{crit}}$ , stripped gas will lead to condensation of coronal gas, so the mass of HI increases over time. Dimensional arguments suggest that the actual mass-loss rate must lie close to  $\alpha_{\text{crit}}$ .

We have used grid-based hydrodynamical simulations of the flight of a cloud to check the analytic arguments. Any hydrodynamical simulation is severely limited by its finite spatial resolution. However, we present evidence from simulations in which radiative cooling has been switched off that our simulations have sufficient resolution to provide reliable estimates of the mass-loss rate. This rate is such that clouds with masses  $\lesssim 1000 M_{\odot}$  (eq. 7) will be totally disrupted before they return to the disc.

Simulations that include radiative cooling confirm the existence of a critical mass-loss rate  $\alpha_{\text{crit}}$  that depends on coronal pressure and metallicity in the expected manner. On account of the restricted resolution of our simulations, we cannot give a definitive value for  $\alpha_{\text{crit}}$  within the local corona. However, we can argue that if the critical mass-loss rate lay above the actual mass-loss rates, the coronal density and metallicity would rise secularly at the expense of the star-forming disc. As a consequence, the  $\alpha_{\text{crit}}$  would decrease until it fell below the actual mass-loss rate. That is, the conditions at the base of the corona have a tendency to adjust until they lead to accretion by the disc.

Although the present model differs materially from that of FB08 in that we envisage the masses of clouds decreasing rather than increasing over time, it seems likely that when the model is used to simulate data cubes for the galaxies studied by FB08, similar agreement with the data will be achieved. This is because FB08 correctly give the dependence on time of both the mass of HI associated with a given cloud, and its velocity centroid. However, a revision of the FB08 models is required to test this conjecture.

The simulations make detailed predictions for what should be seen in studies of the high-latitude HI distribution in the Galaxy. Trails behind clouds should show large gradients in mean velocity that are dominated by hydrodynamical rather than gravitational forces. High-sensitivity data should reveal small quantities of gas distributed around the mean velocity by of order the cloud’s velocity. The trail should be studded by knots of cold gas.

The idea that star-forming discs reach up into the surrounding corona and grab the relatively pristine gas required to sustain their star formation for a Hubble time, makes a good deal of sense cosmologically by explaining how discs can remain star-forming as long as they are not disrupted by a major merger. If after a major merger there are significant streams of cold gas, this gas can seed a new star-forming disc, but in the absence of cold seed-gas, star formation ceases because coronal gas can only condense onto a disc that is already star-forming. Nipoti & Binney (2007) argued that thermal evaporation by coronal gas of filaments of cold gas determines whether a central cusp reforms when an early-type galaxy experiences a major merger. Similarly, when a late-type galaxy experiences a major merger, thermal evaporation of filaments of cold gas can prevent the gas disc reforming.

As a halo proceeds up the clustering hierarchy, the effectiveness of thermal evaporation increases, and at some point a gas disc is prevented from forming after a major merger. Following this event, there is a dramatic reduction in the rate at which coronal gas cools, and the density and X-ray luminosity of the corona increase rapidly. The higher they get, the lower the chance that at the next major merger a cool-gas filament will reach the galactic centre and renew the stellar cusp. Thus there is a direct connection between the process discussed here and the stark contrast in the detectability with X-rays of the coronae of star-forming and early-type galaxies (Rasmussen et al. 2009).

The progressive reduction with cosmic time in the typical halo mass of galaxies making the transition from the blue cloud to the red sequence (“downsizing”), follows from the decrease in the abundance of cold infalling gas with both cosmic time and halo mass-scale that is expected on analytic grounds and observed in *ab-initio* cosmological simulations. It would be interesting to add this idea to semi-analytic models of the evolution of the galaxy population.

## ACKNOWLEDGMENTS

We thank an anonymous referee for his/her valuable comments. Most of the numerical simulations were performed using the BCX system at CINECA, Bologna, with CPU time assigned under the INAF-CINECA agreement 2008-2010. FM gratefully acknowledges support from the Marco Polo program, University of Bologna.

## REFERENCES

- Adelberger K.L., Steidel C.C., Shapley, A.E., Pettini, M., 2003, *ApJ*, 584, 45
- Agertz O., Moore B., Stadel J., Potter D., Miniati F., Read

- J., Mayer L., Gawryszczak A., Kravtsov A., Nordlund A., 2007, MNRAS, 380, 963
- Aumer, M., Binney J., 2009, MNRAS, 397, 1286
- Barnabe M., Ciotti L., Fraternali F., Sancisi R., 2006, A&A, 446, 61
- Benjamin R.A., 2002, in *Seeing Through the Dust* ed. A.R. Taylor, T.L. Landecker, and A.G. Willis, ASP Conference Series, Vol. 276, 201
- Best, P.N.; von der Linden, A.; Kauffmann, G.; Heckman, T.M.; Kaiser, C.R., 2007, MNRAS, 379, 894
- Binney J., 2004, MNRAS, 347, 1093
- Binney J., Nipoti C., Fraternali F., 2009, MNRAS, 397, 1804
- Binney J., Tabor G., 1995, MNRAS, 276, 663
- Birnboim Y., Dekel A. 2003, MNRAS, 345, 349
- Bland-Hawthorn J., Cohen M., 2003, ApJ, 582, 246
- Blanton, M.R., et al., 2003, ApJ, 594, 186 (22 authors)
- Blitz, L.; Spergel, D.N.; Teuben, P.J.; Hartmann, D.; Burton, W.B., 1999, ApJ, 514, 818
- Boomsma R., Oosterloo T.A., Fraternali F., van der Hulst J.M., Sancisi R., 2008, A&A, 490, 555
- Bregman, J.N., Houck, J.C. 1997, ApJ, 485, 159
- Brüns C., Kerp J., Pagels A., 2001, A&A, 370, L26
- Cattaneo A., Dekel A., Devriendt J., Guiderdoni B., Blaizot J., 2006, MNRAS, 370, 1651
- Chiappini C., Matteucci F., Romano D., 2001, ApJ, 554, 1044
- Collins J.A., Benjamin R.A., Rand R.J., 2002, ApJ, 578, 98
- Dinge D., 1997, ApJ, 479, 792
- Fraternali F., 2009, in Andersen J. Bland-Hawthorn J., Nordström B., *The Galaxy Disk in Cosmological Context*, Proc. IAU Symp. 254, p. 255
- Fraternali F., Binney J., 2006, MNRAS, 366, 449 (FB06)
- Fraternali F., Binney J., 2008, MNRAS, 386, 935 (FB08)
- Fukugita M., Peebles P.J.E., 2004, ApJ, 616, 643
- Fukugita M., Peebles P.J.E., 2006, ApJ, 639, 590
- Governato F., Willman B., Mayer L., Brooks A., Stinson G., Valenzuela O., Wadsley J., Quinn T., 2007, MNRAS, 374, 1479
- Heitsch F., Putman M.E., 2009, ApJ, 698, 1485
- Hopkins P.F., Somerville R.S., Cox T.J., Hernquist L., Jogee S., Keres D., Ma C.-P., Robertson B., Stewart K., 2009, MNRAS, 397, 802
- Houck J.C., Bregman J.N., 1990, ApJ, 352, 506
- Jin S., Lynden-Bell D., 2007, MNRAS, 378, L64
- Kalberla P.M.W., Dedes L., 2008, A&A, 487, 591
- Kalberla P.M.W., Burton W.B., Hartmann D., Arnal E.M., Bajaja E., Morras R., Pöppel W.G.L., 2005, A&A, 440, 775
- Kaufmann T., Mayer L., Wadsly J., Stadel J., Moore B., 2006, MNRAS, 370, 1612
- Keres, D.; Katz, N.; Weinberg, D.H.; Davé, R., 2005, MNRAS, 363, 2
- Keres, D.; Katz, N.; Fardal, M.; Davé, R.; Weinberg, D.H., 2009, MNRAS, 395, 160
- Komatsu E., et al., 2009, ApJS, 180, 330 (19 authors)
- Kovac, K.; Oosterloo, T. A.; van der Hulst, J.M., 2009, arXiv0904.2775
- Law D.R., Steidel C.C., Erb D.K., Larkin J.E., Pettini M., Shapley A.E., Wright S.A., 2009, ApJ, 697, 2057
- Lo K.Y., Sargent W.L.W., 1979, ApJ, 227, 756
- Londrillo P., Del Zanna L., 2004, JCoPh, 195, 17
- Marinacci F., Fraternali F., Ciotti L., Nipoti C., 2009, arXiv:0910.0404
- Murray S.D., Whit S.D.M., Blondin J.M., Lin D.N.C., 1993, ApJ, 407, 588
- Nipoti C., Binney J., 2005, MNRAS, 361, 428
- Nipoti C., Binney J., 2007, MNRAS, 382, 1481
- Omma H., Binney J., 2004, MNRAS, 350, L13
- Pagel B.E.J., 1997, *Nucleosynthesis and Chemical Evolution of Galaxies* (Cambridge: CUP)
- Pettini M., Shapley A.E., Steidel C.C., Cuby J.-G., Dickinson M., Moorwood A.F.M., Adelberger K.L., Giavalisco M., 2001, ApJ, 554, 981
- Pisano, D. J.; Barnes, D.G.; Gibson, B.K.; Staveley-Smith, L.; Freeman, K.C.; Kilborn, V.A., 2004, ApJ, 610, 17
- Price D.J., 2008, J.C.Ph., 227, 10040
- Rasmussen J., Sommer-Larsen J., Pedersen K., Toft S., Benson A., Bower R. G., Grove L. F., 2009, ApJ, 697, 79
- Richter P., Westmeier T., Brüns C., 2005, A&A, 442, L49
- Sancisi, R.; Fraternali, F.; Oosterloo, T.; van der Hulst, T., 2008, A&ARv, 15, 189
- Sarazin C.L., 2009, "X-ray Emission from Clusters of Galaxies", Cambridge University Press, Cambridge
- Sembach, K.R.; Wakker, B.P.; Savage, B.D.; Richter, P.; Meade, M.; Shull, J.M.; Jenkins, E.B.; Sonneborn, G.; Moos, H.W., 2003, ApJS, 146, 165
- Shapiro P.R., Field G.B., 1976, ApJ, 205, 762
- Spitzer L., 1956, ApJ, 124, 20
- Spitzer L., Jenkins E.B., 1979, ARA&A, 13, 133
- Strickland, D.K., Heckman T.M., Colbert E.J.M., Hoopes C.G., Weaver K.A., 2004, ApJS, 151, 193
- Sutherland R. S., Dopita M. A., 1993, ApJS, 88, 253
- Twarog B.A., 1980, ApJ, 242, 242
- Vieser W., Hensler G., 2007, A&A, 472, 141
- Wakker B.P., York D.G., Wilhelm R., Barentine J.C., Richter P., Beers T.C., Ivezić Z., Howk J.C., 2008, ApJ, 672, 298
- Westmeier T., Brüns C., Kerp J., 2005, A&A, 432, 937